Mechanochemical Synthesis and Li$^+$ Ion Conductivity of Li$_3$N-based Amorphous Solid Electrolytes

A. HAYASHI, T. OHTOMO, F. MIZUNO and M. TATSUMISAGO

Department of Applied Chemistry, Graduate School of Engineering,
Osaka Prefecture University, Sakai, Osaka 599-8531 (Japan)

E-mail: hayashi@chem.osakafu-u.ac.jp

Abstract

Amorphous solid electrolytes were synthesized in the systems Li$_3$N–P$_2$S$_5$ and Li$_3$N–P *via* mechanochemical route. Amorphous materials were obtained at the compositions with $x = 50$ and 60 in the system xLi$_3$N $\cdot$ (100 $-$ x)P$_2$S$_5$ (mol. %), while crystalline Li$_2$S was obviously formed at the compositions with $x = 70$ and 80. The conductivity increased with increasing Li$_3$N content, and then decreased in the composition range $x > 60$. The highest conductivity of $2.2 \cdot 10^{-5}$ S/cm at room temperature was achieved at the composition with $x = 60$. The formation of insulative Li$_2$S in the compositions with higher Li$_3$N content is responsible for the decrease of conductivity. Li$_3$N was reacted with P instead of P$_2$S$_5$ by milling in order to prevent the formation of Li$_2$S. The obtained materials were basically amorphous, but partially included crystalline materials such as Li$_3$P and Li$_7$PN$_4$. The 80Li$_3$N $\cdot$ 20P (mol. %) material exhibited the highest conductivity of $1.0 \cdot 10^{-5}$ S/cm at room temperature in the system Li$_3$N–P.

INTRODUCTION

The development of highly Li$^+$ ion conducting amorphous solid electrolytes is desired for establishing all-solid-state lithium rechargeable batteries with high safety and reliability. Li$_2$S-based sulphide glassy materials prepared by the melt-quenching method are promising candidates as solid electrolytes for all-solid-state batteries because of their favourable properties of high Li$^+$ conductivity over 10^{-4} S/cm at room temperature and wide electrochemical window [1–3].

The sulphide amorphous solid electrolytes were also synthesized *via* mechanochemical route [4]. The preparation procedure using a high-energy ball mill apparatus is very useful for obtaining amorphous fine powders, which achieve close contact between electrolyte and electrode in solid-state batteries. The Li$_2$S–SiS$_2$ amorphous materials prepared by milling for several hours exhibited the conductivity of 10^{-4} S/cm at room temperature [5, 6]. Solid-state NMR measurements revealed that the local structure around silicon atoms of the Li$_2$S–SiS$_2$ materials milled for 20 h was almost the same as that of the corresponding melt-quenched glasses.

In the case of using Li$_3$N as a lithium source instead of Li$_2$S, Li$^+$ conducting amorphous materials were prepared in the system Li$_3$N–SiS$_2$ by milling for very short periods such as 20 min (the reaction would be based on "compulsion reaction") [7]. The 40Li$_3$N $\cdot$ 60SiS$_2$ (mol. %) material showed excellent properties such as high conductivity of $2.7 \cdot 10^{-4}$ S/cm at room temperature, unity of Li$^+$ ion transference number, and wide electrochemical window of 10 V.

On the other hand, sulphide amorphous electrolytes with different glass-formers such as P$_2$S$_5$ [8], Al$_2$S$_3$ [9], and GeS$_2$ [10] instead of SiS$_2$ were also synthesized by milling. In particular, the Li$_2$S–P$_2$S$_5$ amorphous materials are one of the excellent solid electrolytes; the conductivity can be further improved by crystallization of the amorphous sample [11] and all-solid-state batteries with the Li$_2$S–P$_2$S$_5$ solid electrolytes exhibited excellent cycling performance [12]. The combination of Li$_3$N as a lithium source and P$_2$S$_5$ as a glass former is a most attractive system for solid electrolytes.

In the present study, the Li_3N-based amorphous solid electrolytes were synthesized in the system $Li_3N-P_2S_5$ by mechanical milling using a planetary ball mill apparatus. The Li_3N-P materials using elemental P instead of P_2S_5 were also prepared. Structure and electrical properties of the obtained materials were investigated.

EXPERIMENTAL

Reagent-grade Li_3N and P_2S_5 or P (red phosphorus) powders were used as starting materials for sample preparation. The Li_3N and P_2S_5 powders were crystalline and P was amorphous. The mechanical milling treatment was carried out for the batch (1 g) of the mixed materials placed into a stainless steel pot (volume of 45 ml) with 10 stainless steel balls (10 mm in diameter) using a high-energy planetary ball mill apparatus (Fritsch Pulverisette 7). The rotation speed was fixed at 370 rpm and all processes were conducted at room temperature in a dry Ar-filled glove box.

X-ray diffraction (XRD) measurements were carried out using a Mac-Science M18XHF[22]-SRA diffractometer with CuK_α radiation for the obtained materials. The sample was sealed in an Ar-filled container with the beryllium windows.

The electrical conductivity of the samples was measured by using AC impedance methods. The powder samples were pelletized by cold pressing at 3700 kg/cm^2 and carbon paste was painted on both sides of the pellet to serve as electrodes. The electrical conductivity of the pellet was measured in a dry Ar atmosphere from 10 Hz to 8 MHz with an impedance analyzer (Model 1260, Solartron) in the temperature range of 25−180 ºC.

RESULTS AND DISCUSSION

Figure 1 shows the X-ray diffraction (XRD) patterns of powder samples of $50Li_3N \cdot 50P_2S_5$ (mol. %) with different milling periods. Numbers in the Figure mean the milling periods of time. Diffraction peaks due to the crystals of Li_3N and P_2S_5 are observed in the powder mixture without mechanical milling (0 h). As the milling period increases, the intensity of those crystalline peaks decreases and the halo pat-
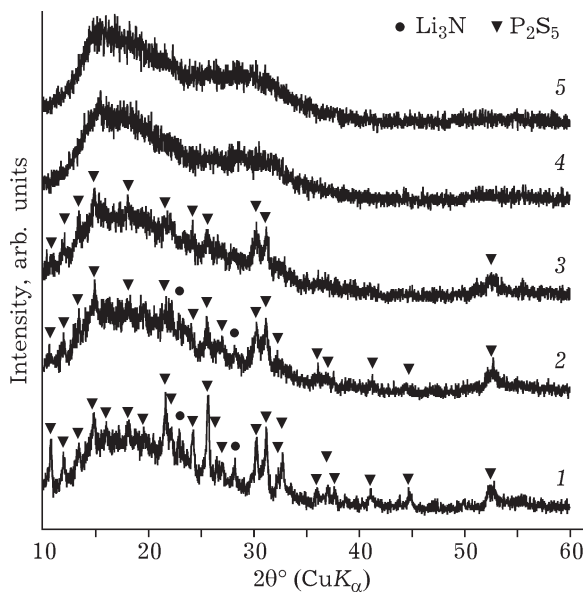

Fig. 1. XRD patterns of the $50Li_3N \cdot 50P_2S_5$ (mol. %) sample prepared by mechanical milling for different periods, h: 0 (*1*), 1 (*2*), 5 (*3*), 10 (*4*), 20 (*5*).

tern becomes dominant. The peaks due to Li_3N disappear after milling for 5 h, and the peaks due to P_2S_5 disappear after milling for 10 h. Amorphization gradually proceeds during milling, and the amorphous material is obtained after milling for at least 10 h.

Figure 2 shows the XRD patterns of the $xLi_3N \cdot (100 - x)P_2S_5$ (mol. %) ($x = 50, 60, 70$, and 80) samples mechanically milled for 20 h. The samples of $x = 50$ and 60 basically show

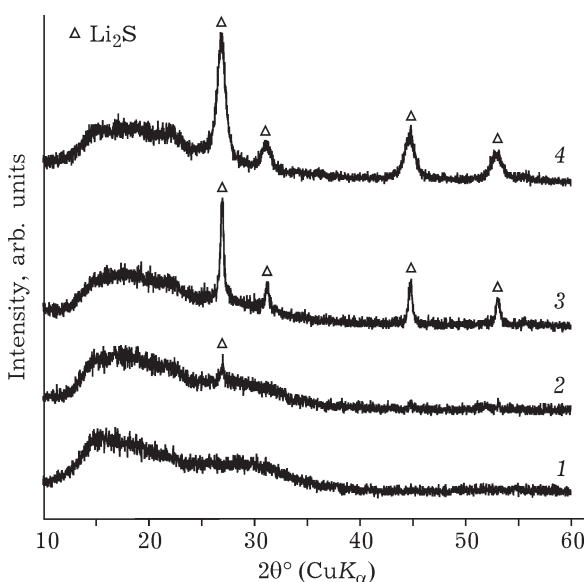Fig. 2. XRD patterns of the $xLi_3N \cdot (100 - x)P_2S_5$ samples prepared by mechanical milling for 20 h. x value: 50 (*1*), 60 (*2*), 70 (*3*), 80 (*4*).

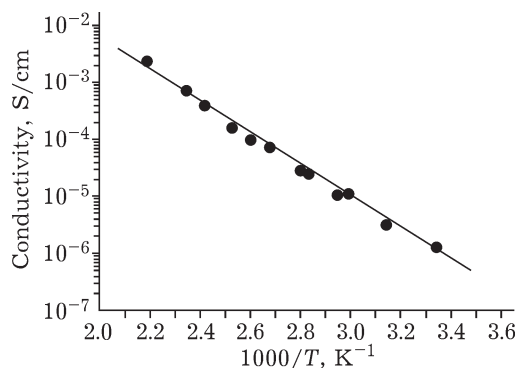Fig. 3. Temperature dependence of conductivity of the 50Li$_3$N · 50P$_2$S$_5$ (mol. %) sample prepared by mechanical milling for 20 h.

halo patterns on XRD measurements, suggesting that the obtained materials are amorphous. The peaks due to Li$_2$S crystal are obviously observed for the samples of x = 70 and 80. The reaction between Li$_3$N and P$_2$S$_5$ by mechanical milling produces Li$_2$S at the higher Li$_3$N compositions.

Figure 3 shows the temperature dependence of electrical conductivity of the pelletized 50Li$_3$N · 50P$_2$S$_5$ amorphous sample prepared by milling for 20 h. The conductivities of the sample follow the Arrhenius equation and the activation energy (E_a) for conduction was calculated from the slope. Figure 4 shows the composition dependence of conductivity at 25 °C (σ_{25}) and the activation energy (E_a) for conduction of the xLi$_3$N · (100 − x)P$_2$S$_5$ samples prepared by milling for 20 h. The conductivity increases with increasing Li$_3$N content, an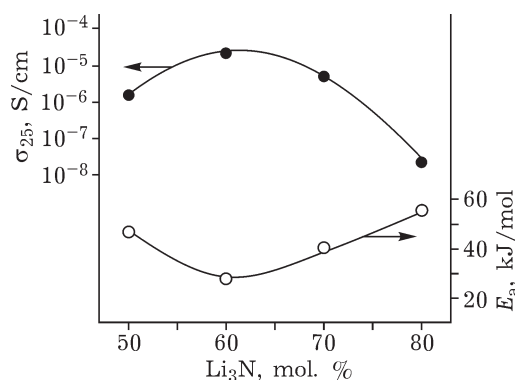d then decreases in the composition range x > 60. The highest conductivity of 2.2 · 10^{-5} S/cm at room temperature is achieved at the composition with x = 60. The composition dependence of E_a corresponds to that of σ_{25} and the minimum E_a of 28 kJ/mol is obtained at the composition with x = 60. The increase in Li$_3$N content improves conductivity because of increasing Li$^+$ carrier concentration in amorphous matrix. On the other hand, the formation of insulative Li$_2$S in the compositions with higher Li$_3$N content is responsible for the decrease of conductivity.

Li$_3$N was then reacted with elemental P instead of P$_2$S$_5$ by milling in order to prevent the formation of Li$_2$S. Figure 5 shows the XRD patterns of the yLi$_3$N · (100 − y)P (mol. %) (y = 50, 60, 70 and 80) samples mechanically milled for 20 h. The obtained materials were basically amorphous, but partially included crystalline materials formed during milling. The Li$_3$P crystal is precipitated at the compositions y = 50 and the Li$_7$PN$_4$ crystal is mainly precipitated at the compositions y = 60 and 70. The Li$_3$N phase as a starting material partially remains at the composition y = 80. It is revealed that phosphide and phosphorus nitride compounds can be synthesized by mechanochemical route using the starting materials Li$_3$N and P.

Since the lithium phosphorus nitride, Li$_7$PN$_4$, is formed in the milled materials, the P−N bonds would also be formed in amorphous matrix. The formation of lithium phosphide Li$_3$P indicates that elemental P is reduced from P^0
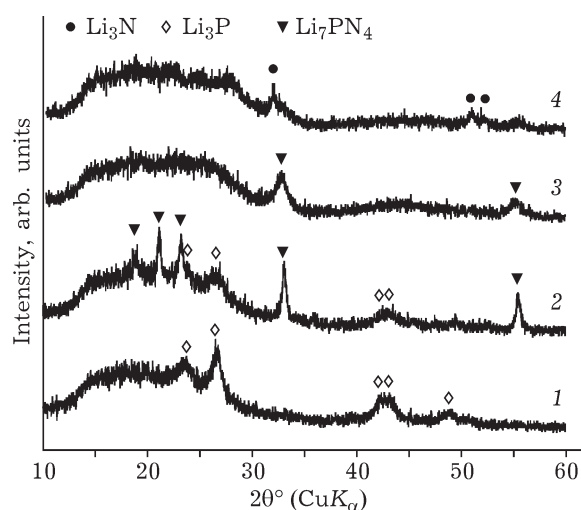

Fig. 4. Composition dependence of conductivities at 25 °C (σ_{25}) and activation energies for conduction (E_a) for the xLi$_3$N · (100 − x)P$_2$S$_5$ (mol. %) (x = 50, 60, 70 and 80) samples prepared by mechanical milling for 20 h.

Fig. 5. XRD patterns of the yLi$_3$N · (100 − y)P (mol. %) samples prepared by mechanical milling for 20 h. y value: 50 (1), 60 (2), 70 (3), 80 (4).
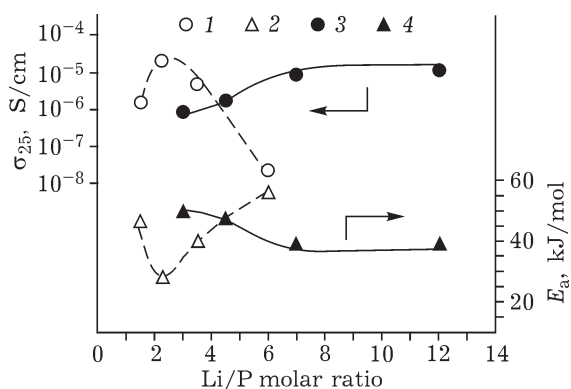
Fig. 6. Composition dependence of conductivities at 25 °C (σ_{25}) and activation energies for conduction (E_a) of the $Li_3N-P_2S_5$ and Li_3N-P samples prepared by mechanical milling for 20 h: *1, 2* − σ_{25} and E_a of the $Li_3N-P_2S_5$ samples, respectively; *3, 4* − σ_{25} and E_a of the Li_3N-P samples, respectively.

to P^{3-} and then N_2 gas would be generated during milling.

Figure 6 shows the composition dependence of conductivities at 25 °C (σ_{25}) and activation energies for conduction (E_a) of the Li_3N-P samples prepared by mechanical milling for 20 h. The data of the $Li_3N-P_2S_5$ milled sample are also shown. The conductivity increases with increasing Li_3N content in the system Li_3N-P; the $80Li_3N \cdot 20P$ material exhibits the highest conductivity of $1.0 \cdot 10^{-5}$ S/cm at room temperature.

The conductivity of the milled materials depends on the Li^+ concentration in amorphous matrix and the precipitated crystal phases. The Li_3P crystal was reported to show high conductivity of $7.0 \cdot 10^{-4}$ S/cm at room temperature [13], while the Li_7PN_4 crystal exhibited low conductivity of $1.4 \cdot 10^{-7}$ S/cm [14]. The sample $x = 50$ partially included the Li_3P phase, but its conductivity is in the order of 10^{-6} S/cm. Both insufficient crystallinity of Li_3P and low Li^+ concentration would be the reason for low conductivity of the sample $x = 50$. On the other hand, the conductivity increases with an increase in x ($x > 60$) in spite of the presence of less conductive Li_7PN_4 phase because the Li^+ concentration in amorphous matrix increases.

The conductivities of Li_3N-based amorphous materials were compared with those of the $Li_2S-P_2S_5$ amorphous materials. The $60Li_3N \cdot 40P_2S_5$ amorphous material (Li/P = 2.25) showed the maximum conductivity of $2.2 \cdot 10^{-5}$ S/cm at room temperature. The higher conductivity of

$5 \cdot 10^{-5}$ S/cm was reported for the $70Li_2S \cdot 30P_2S_5$ amorphous material with almost the same Li content (Li/P = 2.33) [8]. The incorporation of nitrogen atoms into sulphide amorphous matrix is one of the reasons for decreasing conductivity in the Li_3N-based materials. The use of P instead of P_2S_5 results in preventing the formation of insulative Li_2S crystal and increasing Li^+ concentration and, however, the conductivity is still low (in the order of 10^{-5} S/cm). It is assumed that the Li−P−N amorphous matrix is less conductive than the Li−P−S amorphous matrix.

The conductivity of the $70Li_2S \cdot 30P_2S_5$ amorphous material was increased by heat treatment at the crystallization temperature, and the obtained glass ceramic electrolyte exhibited high conductivity of over 10^{-3} S/cm at room temperature [11]. The precipitation of superionic $Li_7P_3S_{11}$ metastable phase is responsible for the high conductivity. The $60Li_3N \cdot 40P_2S_5$ amorphous sample was crystalized at 290 °C (just over the crystallization temperature) and the ambient temperature conductivity of the sample was also increased from $2.2 \cdot 10^{-5}$ to $9.1 \cdot 10^{-5}$ S/cm, which is, however, lower than the conductivity of the $Li_2S-P_2S_5$ glass ceramics. This is because less conductive $Li_4P_2S_6$ and unknown phases were precipitated in the $Li_3N-P_2S_5$ glass ceramic material.

CONCLUSIONS

Amorphous solid electrolytes were synthesized in the systems $Li_3N-P_2S_5$ and Li_3N-P *via* mechanochemical route. Amorphous materials were obtained at the compositions with $x = 50$ and 60 in the system $xLi_3N \cdot (100 − x)P_2S_5$, while crystalline Li_2S was obviously formed at the compositions with $x = 70$ and 80. The conductivity increased with increasing Li_3N content, and then decreased in the composition range $x > 60$. The highest conductivity of $2.2 \cdot 10^{-5}$ S/cm at room temperature was achieved at the composition with $x = 60$. The formation of insulative Li_2S in the compositions with higher Li_3N content is responsible for the decrease of conductivity. The materials obtained by milling for the mixture of Li_3N and P, were basically amorphous, but partially included crystalline

materials such as Li$_3$P and Li$_7$PN$_4$. The 80Li$_3$N $\cdot$ 20P (mol. %) material exhibited the highest conductivity of $1.0 \cdot 10^{-5}$ S/cm at room temperature in the system Li$_3$N−P.

Acknowledgements

REFERENCES

1 R. Mercier, J. P. Malugani, B. Fahys and G. Robert, *Solid State Ionics*, 5 (1981) 663.

2 A. Pradel and M. Ribes, *Ibid.*, 18/19 (1986) 351.

3 T. Minami, A. Hayashi and M. Tatsumisago, *Ibid.*, 136−137 (2000) 1015.

4 M. Tatsumisago, *Ibid.*, 175 (2004) 13.

5 H. Morimoto, H. Yamashita, M. Tatsumisago and T. Minami, *J. Am. Ceram. Soc.*, 82 (1999) 1352.

6 H. Yamashita, A. Hayashi, H. Morimoto *et al.*, *J. Ceram. Soc. Jpn.*, 108 (2000) 973.

7 K. Iio, A. Hayashi, H. Morimoto *et al.*, *Chem. Mater.*, 14 (2002) 2444.

8 A. Hayashi, S. Hama, H. Morimoto *et al.*, *J. Am. Ceram. Soc.*, 84 (2001) 477.

9 A. Hayashi, T. Fukuda, H. Morimoto *et al.*, *J. Mater. Sci.*, 39 (2004) 5125.

10 H. Yamamoto, N. Machida and T. Shigematsu, *Solid State Ionics*, 175 (2004) 707.

11 F. Mizuno, A. Hayashi, K. Tadanaga and M. Tatsumisago, *Adv. Mater.*, 17 (2005) 918.

12 F. Mizuno, A. Hayashi, K. Tadanaga *et al.*, *Chem. Lett.*, (2002) 1244.

13 G. Nazri, *Solid State Ionics*, 34 (1989) 97.

14 W. Schnick and J. Luecke, *Ibid.*, 38 (1990) 271.